

Role of additives in bright zinc deposition from cyanide free alkaline baths

SHANMUGASIGAMANI and MALATHY PUSHPAVANAM*

Central Electrochemical Research Institute, Karaikudi 630 006, TamilNadu, India

(*author for correspondence, e-mail: malathypush@yahoo.com)

Received 17 October 2004; accepted in revised form 9 September 2005

Key words: Alkaline non-cyanide Bright zinc plating, cathode current efficiency, cyclic voltammetry, Hull cell studies, thickness distribution

Abstract

A new additive formulation for non-cyanide alkaline zinc baths was identified after experiments with various additives. Polyvinyl alcohol addition was found to be the best primary additive of those tested. The secondary additives selected belonged to the aldehyde group. The selection of the additives was made based on Hull cell, cathode current efficiency and throwing power studies. Thickness measurements at various points on a cathode indicated uniform thickness distribution. XRF showed uniform deposition. SEM examination indicated a fine-grained deposit structure. Finally, the influence of each additive was studied using cyclic voltammetry.

1. Introduction

Electrodeposited zinc coatings have found widespread use as sacrificial protection for steel substrates [1]. Several plating electrolytes are used in industry, notably those based on cyanide, alkaline non-cyanide, acid sulphate and neutral chloride formulations [2]. The use of cyanide zinc solutions, in spite of their operator friendly nature, is being discouraged due to health and environmental pollution hazards as well as high effluent treatment costs [3]. A comprehensive examination of different zinc plating lines, including those based on cyanide in various concentrations, and the alkaline zincate bath by Geduld, estimates the total cost of production ratios to be 2.36, 1.48, 1.1 and 1.0 for high cyanide, mid cyanide, low cyanide and zincate baths respectively [4].

Alkaline non-cyanide zinc baths are a logical development in the effort to produce a non-toxic cyanide free zinc electrolyte. Initially these baths were considered as able to give only dark, spongy or powdery deposits over normal plating current densities and it was necessary to replace the complexing effect of cyanide ions by other complexing agents like EDTA, gluconate, tartrate and triethanolamine [4]. However, this created new effluent problems. The modern alkaline non-cyanide baths make use of organic addition agents to produce commercially acceptable bright deposits.

A number of organic additives are reported in the literature, which fall into two categories—the carrier and the brightener. Generally, the carrier additive would enable grain refinement and the brightener additive would have a complementary effect in producing bright

deposits. Since, most of the formulations are proprietary in nature, a detailed study to explore a viable combination of the additives is essential [5–8].

The present study deals with the development of a suitable brightener formulation for an alkaline non-cyanide zinc bath.

2. Experimental

The alkaline non-cyanide zinc bath was prepared by using ZnO and NaOH (Base Electrolyte = BE) (Table 1). Due pretreatments were given to the bath to remove the metallic and organic impurities [4, 9]. Hull cell studies were made using a 267 ml cell at current $I=1$ A and duration $t=10$ min [10]. Suitably pretreated mild steel cathode panels and plating grade zinc anodes were used. Polyvinyl alcohol (PVA) [4–5, 8], Benzyl chloride–Nicotinic acid derivative (BCNA) [2, 11], Epichlorohydrin (ECH) [12–14], Tetra Ethylene Pent Amine (TEPA) [4, 13], Polypropylene Imine (PPI) [15] and Rochelle salt (sodium potassium tartrate) (RS) [16] were tested as carrier additives. The brightener additives tested included Piperonal (PIP) [14], Anisaldehyde(ANI)[13–15], Veratraldehyde(VER) [13–14 and 17] and Acetonyl acetone (ACA). All chemicals used were of Laboratory Grade, supplied by Merck or

Table 1. Bath composition used

BE	Concentration (g l^{-1})
Zinc oxide	9–12
NaOH	90–120

Fischer. Cathodic Current Efficiencies (CCE) were estimated at different current densities from the increase in mass of the deposits after deposition applying a known quantity of electricity. The operating current density range, deposit brightness etc. were taken as the main criteria for selecting the additives. Thickness on the Hull cell patterns was measured using X-ray fluorescence spectroscopy (XRF, CMI, XRX series USA) after dividing the panel into five equal segments to determine the throwing power. The results obtained were substantiated with throwing power estimation using a Haring and Blum cell with a metal distribution ratio of 5 applying Field's formula.

The effect of different additives on the cathode polarization was galvanostatically evaluated using a steel cathode ($S=1\text{ cm}^2$), platinum anode and a saturated calomel (SCE) reference electrode [18] in a three-necked

H-type cell. Constant current was applied in small increments using a controlled power supply unit and corresponding potentials were recorded after allowing sufficient time to reach the steady state. The additive influence was also evaluated by cyclic voltammetry using a Potentiostat (Wenking, Model 81, Germany) connected to a function generator (Wenking, Model SG 79) and a X-Y-t recorder. The same cell set up as mentioned above was used for this study. Potentials were scanned between -1200 mV to -1700 mV at a scan rate of 10 mV s^{-1} .

Structural examination of the deposits was made using Scanning Electron Microscopy (SEM).

3. Results

Figure 1a-f shows the Hull cell patterns obtained in the presence of carrier additives like Rochelle salt, Polyvinyl

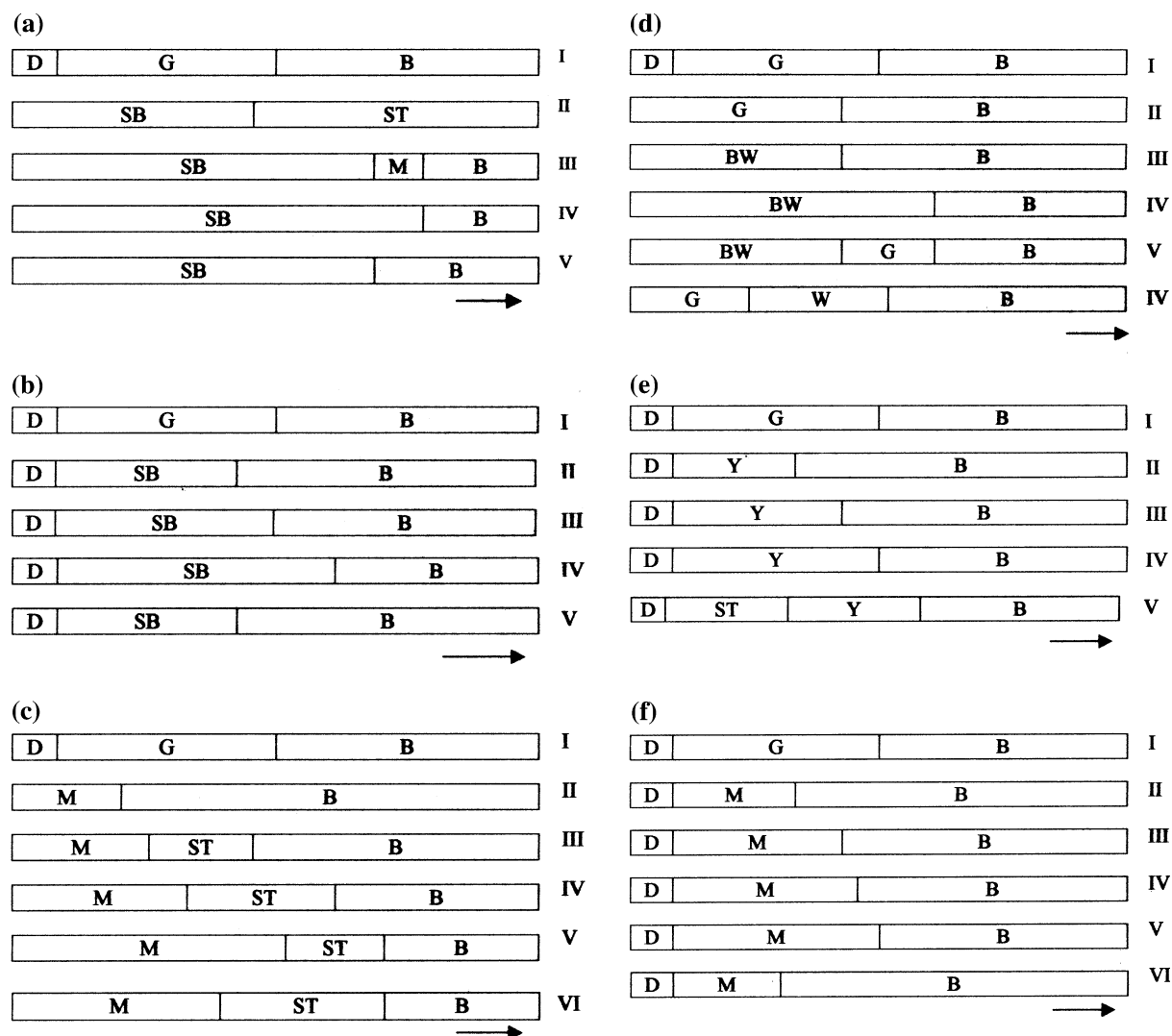


Fig. 1. (a) Hull cell pattern obtained from BE containing PVA with various concentrations. (I) BE; BE+PVA (II) 0.5 g l^{-1} (III) 1.0 g l^{-1} (IV) 1.5 g l^{-1} (V) 2 g l^{-1} ; (b) Hull cell pattern obtained from BE containing RS. (I) BE; BE+RS (II) 1.5 g l^{-1} (III) 32.5 g l^{-1} (IV) 35 g l^{-1} (V) 37.5 g l^{-1} (VI) 40 g l^{-1} ; (c) Hull cell pattern obtained from BE containing TEPA. (I) BE; BE + TEPA (II) 0.25 g l^{-1} (III) 0.5 g l^{-1} (IV) 1.0 g l^{-1} (V) 1.5 g l^{-1} (VI) 2.0 g l^{-1} ; (d) Hull cell pattern obtained from BE containing BCNA. (I) BE; BE+ BCNA (II) 7.5 g l^{-1} (III) 8 g l^{-1} (IV) 8.5 g l^{-1} (V) 9 g l^{-1} (VI) 9.5 g l^{-1} ; (e) Hull cell pattern obtained from BE containing PPI. (I) BE; BE+ PPI (II) 0.6 g l^{-1} (III) 1.35 g l^{-1} (IV) 2 g l^{-1} (V) 2.5 g l^{-1} ; (f) Hull cell pattern obtained from BE containing ECH. (I) BE; BE+ ECH (II) 1.0 g l^{-1} (III) 1.5 g l^{-1} (IV) 2.0 g l^{-1} (V) 2.5 g l^{-1} (VI) 3.0 g l^{-1} . Code For Hull Cell Figures: D – Dull; G – grey; B–black; M–matte; Y–Yellow filmed; W – white; SB – Semi bright; BR – Bright; MB – Mirror bright; ST – Streaky; BST – Bright streaky.

alcohol, Poly propylene imine, Epichlorohydrin, Benzyl chloride + Nicotinic acid Derivative and Tetra Ethylene Pent amine. PPI yielded deposits with an unattractive yellow tinge. ECH and TEPA gave rise to only matte deposits. BCNA yielded white deposits but involved a cumbersome preparative procedure. Only Rochelle salt and PVA yielded semi bright deposits. But, considering the wide operating window and low concentration of the complex, PVA was selected as the best carrier additive.

Figure 2a–d shows the effect of various brightener additives in the presence of PVA on the Hull cell patterns produced from a zinc bath. All the four-brightener additives improved the deposit properties. Their difference in performance could be compared only on the basis of the degree of brightness produced. While ANI produced bright deposits ACA produced semibright deposits, PIP and VER produced mirror bright deposits over a wide spectrum of current density indicating that the last two additives are best suited. Of these two, selection was made based on the cathode current efficiency, throwing power and the nature of deposits produced [4].

Figure 3 shows the comparison of CCE for the plain zinc bath and the zinc bath with additives at different current densities. For the plain zinc bath the CCE ranged from 42 to 58%, the maximum being at 2 A dm^{-2} . Addition of PVA improved the CCE, though the trend remained almost the same. Addition of the aldehydes changed the behaviour such that the CCE was almost unchanged up to 2 A dm^{-2} and thereafter declined. PIP showed the maximum CCE ranging from 76 to 84%.

Figure 4 shows the thickness of the zinc deposits obtained on a segmented Hull cell cathode. The variation of thickness with current density is an indication of throwing power. The lower the A/B value, (ratio of thickness at high current density to that at low current density) the higher is the throwing power of the system. As shown in Table 2, the A/B value for the PVA + PIP system is lower than that for the PVA + VER system and the PVA + ANI system shows the highest value. The A–B value also shows a similar trend.

The throwing power values obtained using Haring & Blum cell are depicted in Figure 5. The values obtained follow a similar trend as observed in Figure 4.

Figure 6 shows the cathodic polarization curves wherein the presence of various additives causes inhibition of various degrees to zinc deposition. Addition of PVA caused a considerable shift of the I–E curves towards more negative potential. When aldehydes were added to this electrolyte a further shift in the negative direction was recorded and the extent of the shift was minimum for PVA + PIP and maximum for PVA + ANI.

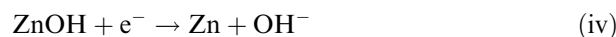
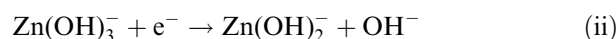
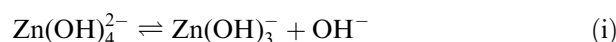
Figure 7 shows the SEM micrographs of zinc deposits obtained with and without additives. Figure 7a shows the micrograph obtained from a plain bath and Figure 7b with the addition of PVA. A leaf like surface film was observed, though considerable grain refinement was observed beneath the film. Figure 7c and d are the micrographs obtained with PVA + PIP and PVA + VER, respectively. While the former produced a uniform fine-

grained structure, the latter led to a heterogeneous structure, though fine grained.

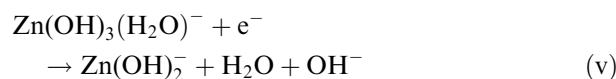
Figure 8 shows the cyclic voltammogram of zinc deposition obtained from the alkaline bath. The voltammogram showed two cathodic peaks p_1 and p_2 and an anodic peak. Addition of PVA shifted p_1 and p_2 to less negative potentials and suppressed both I_{p_1} and I_{p_2} (Figure 8a). Addition of aldehydes generally shifted the E_{p_1} to more negative and E_d (Deposition potential) and E_{p_2} values to less negative values than that of BE + PVA electrolyte. I_{p_1} , which became smaller with the addition of PVA to BE, showed a marginal decrease in the presence of aldehydes and I_{p_2} also decreased in the order PVA + PIP > PVA + VER > PVA + ANI (Figure 8b–d). The peak potential and current values are summarized in Table 3.

4. Discussion

The following four-step reaction path has been proposed [19] for the deposition of zinc from zincate solution.



with reaction (ii) as the rate determining step. Since Zn^{2+} prefers to exist as a tetra or hexa-coordinate species, the coordinated Zn(OH)_3^- is more likely to exist as $\text{Zn(OH)}_3(\text{H}_2\text{O})^-$, thus step (ii) becomes



Since the rate of reaction (v) is still generally faster than the rate of transport of electro active species to the site of discharge, powdery non-adherent deposits result. Thus in order to achieve bright, useful deposits the rate of reaction (v) must be reduced. Though some form of control can be achieved by increasing the hydroxide concentration, this can only be achieved with organic additives, which either modify step (ii/v) or bring about selective deposition [19].

The carrier additives are added to modify the above steps. Among a number of carrier additives tested, PVA proved to be the best. Owing to the polarity of the carbon–oxygen bond, it is possible for this material to be present in significant amounts in the cathode film, forming a weak physical barrier that hinders zinc deposition. It is also possible that PVA replaces the H_2O present in the complex $\text{Zn(OH)}_3^- \text{H}_2\text{O}$. That is

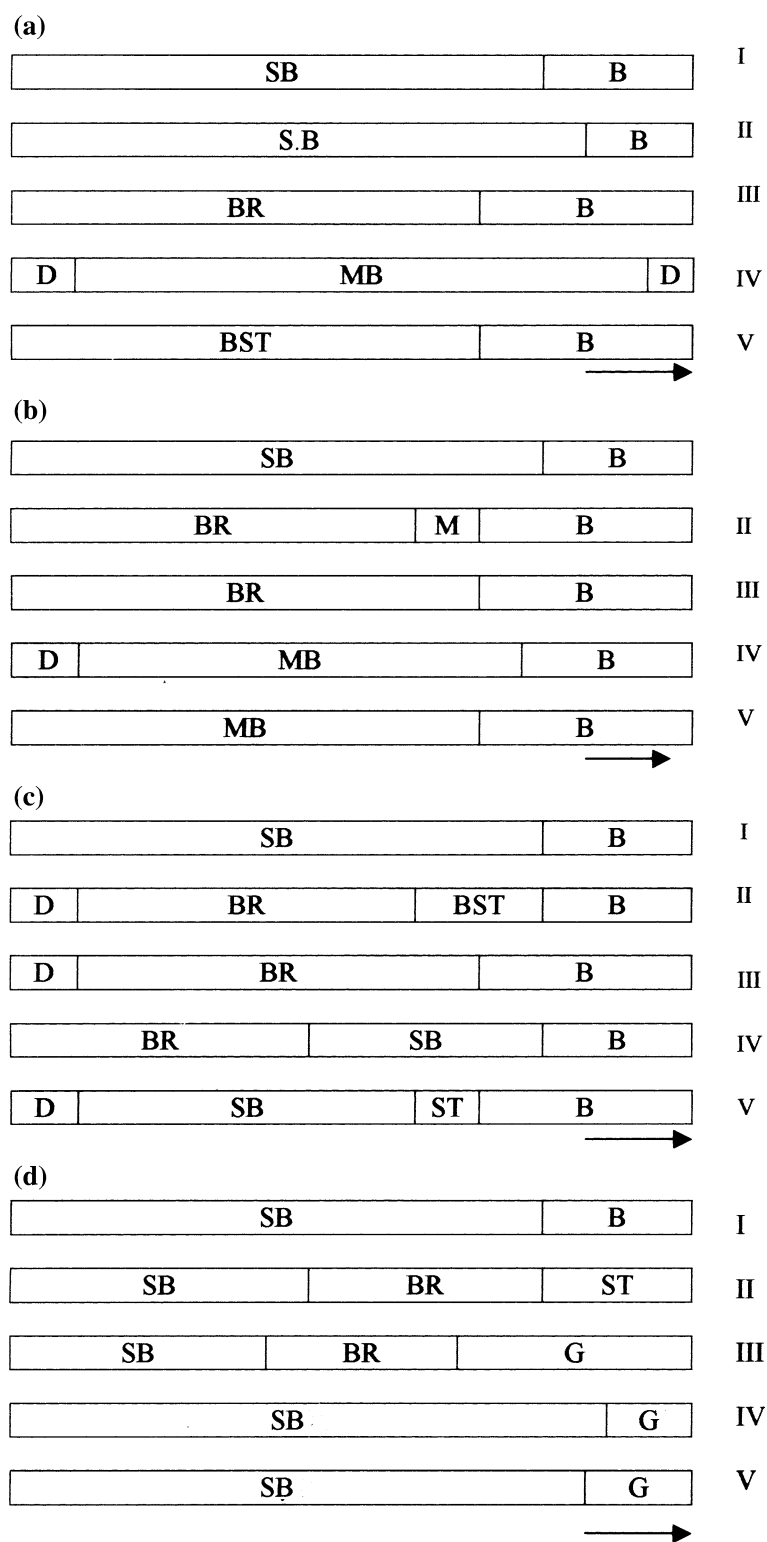


Fig. 2. (a) Hull cell pattern obtained from BE containing PVA with PIP. BE+PVA 1.5 g l⁻¹; BE+PVA+PIP (II) 0.6 g l⁻¹ (III) 0.8 g l⁻¹ (IV) 1.0 g l⁻¹ (V) 1.5 g l⁻¹; (b) Hull cell pattern obtained from BE containing PVA with VER. BE+PVA 1.5 g l⁻¹; BE+PVA+VER (II) 0.2 g l⁻¹ (III) 0.3 g l⁻¹ (IV) 0.4 g l⁻¹ (V) 0.6 g l⁻¹; (c) Hull cell pattern obtained from BE containing PVA with ANI. (I) BE+PVA 1.5 g l⁻¹; BE+PVA+ANI (II) 0.08 g l⁻¹ (III) 0.2 g l⁻¹ (IV) 0.6 g l⁻¹ (V) 0.8 g l⁻¹; (d) Hull cell pattern obtained from BE containing PVA with ACA. (I) BE+PVA 1.5 g l⁻¹; BE+PVA+ACA (II) 0.4 g l⁻¹ (III) 0.6 g l⁻¹ (IV) 0.8 g l⁻¹ (V) 1.0 g l⁻¹. Code For Hull Cell Figures: D – Dull; G – grey; B–black; M–matte; Y–Yellow filmed; W – white; SB – Semi bright; BR – Bright; MB – Mirror bright; ST – Streaky; BST – Bright streaky.

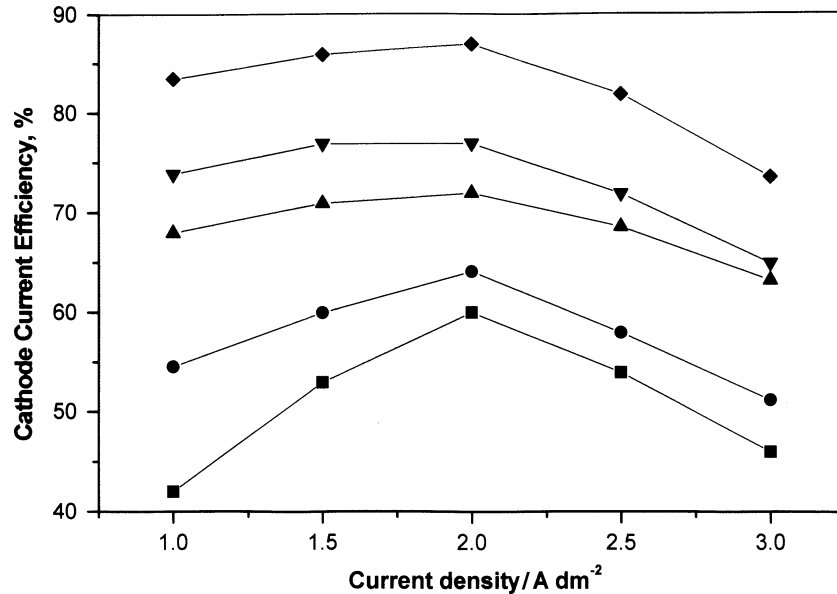


Fig. 3. Effect of various additives in cathode current efficiency of zinc deposition. ■BE ●BE+PVA (1.5 g l⁻¹) ▲ BE+PVA+ANI (0.2 g l⁻¹) ▼BE+PVA+VER (0.4 g l⁻¹) ◆ BE+PVA+PIP (1.0 g l⁻¹).

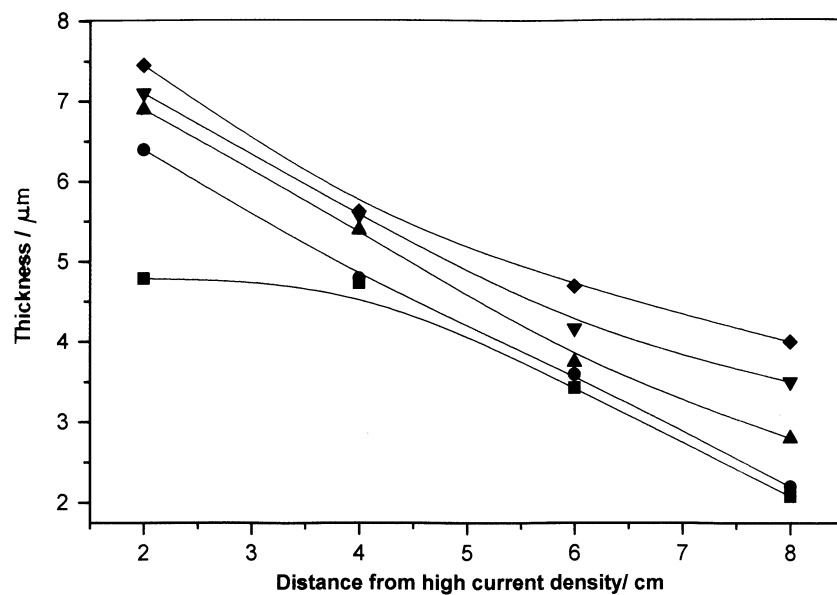
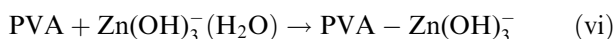
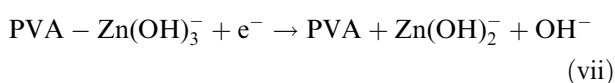


Fig. 4. Thickness of zinc deposits obtained from Hull cell cathode. ■BE ●BE+PVA (1.5 g l⁻¹) ▲BE+PVA+ANI (0.2 g l⁻¹) ▼BE+PVA+VER (0.4 g l⁻¹) ◆ BE+PVA+PIP (1.0 g l⁻¹).



In this way the PVA chains can retain zinc hydroxyl anions and control the speed of the rate-determining step, which would then become



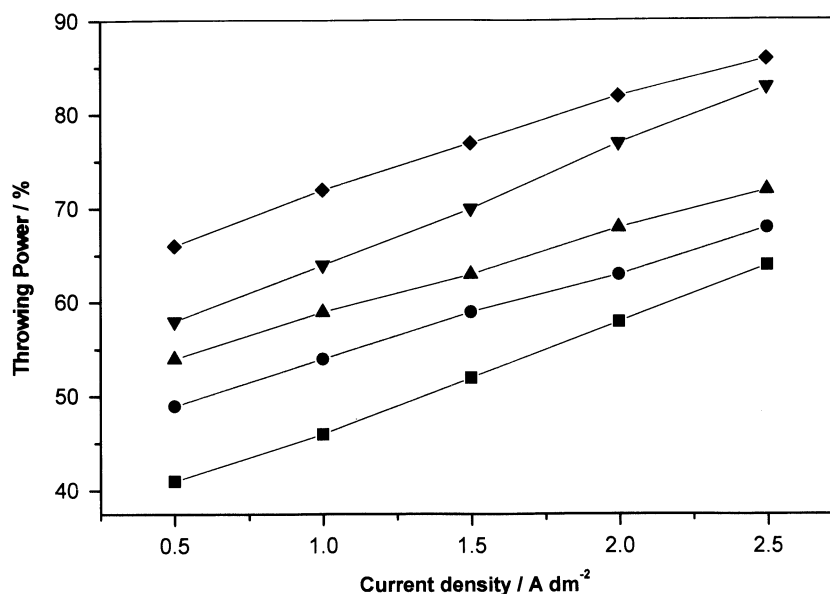
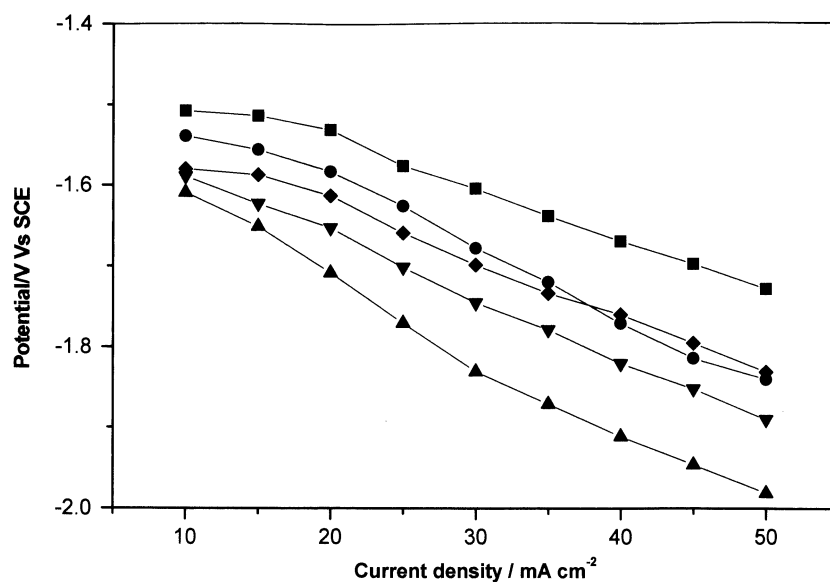
Assuming reaction (vii) as being much slower than (v), because of the energy needed to break the PVA complex, would explain the grain refining properties of PVA [10]. As indicated by Figure 7, addition of PVA enables grain refinement of the deposits but at the same

time, produces a leaf like polymeric surface film. Due to the formation of compact deposits, as against the mossy or spongy deposits, the cathode efficiency increases slightly.

To obtain bright zinc from this bath additional organic brighteners are needed in addition to PVA. These organic brighteners are smaller molecules having unsaturated and polar characteristics by which they are attracted to the cathode and influence deposition. The roll of brightener additives is to further refine the structure or produce leveling by selective adsorption. Only, in the presence of the brightener additive is the surface film formed by PVA eliminated. The Hull cell

Table 2. Metal distribution on a Hull cell panel

Bath	Deposit thickness/ μm		Difference (A-B)/ μm	Ratio (A/B)
	at 3.5 A dm^{-2}	at 0.4 A dm^{-2}		
BE	4.79	2.08	2.71	2.3
BE + PVA	6.4	2.2	4.2	2.9
BE + PVA + PIP	7.45	4.0	3.45	1.86
BE + PVA + VER	7.1	3.5	3.45	2.02
BE + PVA + ANI	6.9	2.8	4.1	2.46

Fig. 5. Throwing power by Haring & Blum cell. ■BE ●PVA (1.5 g l^{-1}) ▲PVA + PIP (1 g l^{-1}) ▼PVA + VER (0.4 g l^{-1}) ◆PVA + ANI (0.2 g l^{-1}).Fig. 6. Polarization behaviour of zinc deposition. ■BE ●BE + PVA (1.5 g l^{-1}) ▲BE + PVA + VER (0.4 g l^{-1}) ▼BE + PVA + ANI (0.2 g l^{-1}) ◆BE + PVA + PIP (1.0 g l^{-1}).

patterns clearly indicate that PIP or VER are good brightener additives. But, the former is better than the latter in terms of cathode efficiency and throwing power.

Cathodic polarization curves distinctly show the inhibitive effect caused by PVA probably forming the chain as shown in reactions (vi) and (vii). The addition

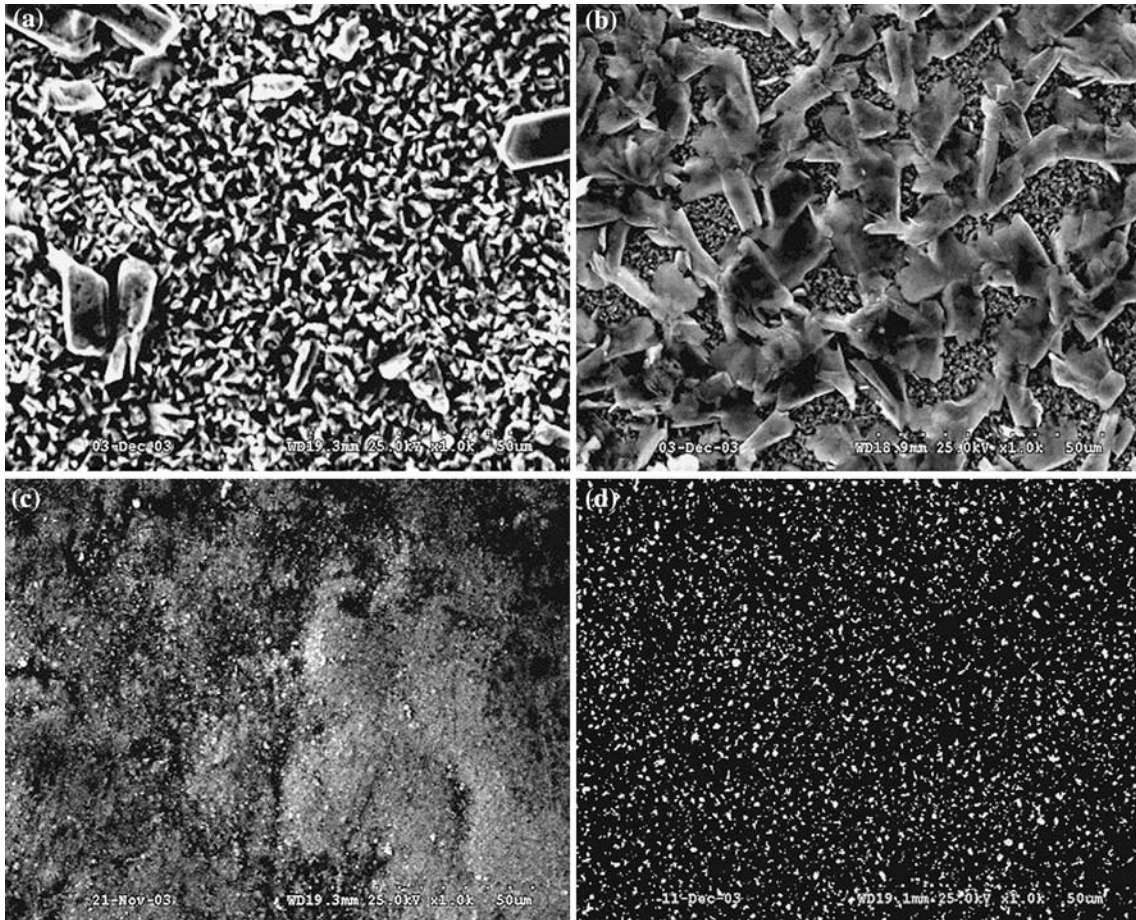


Fig. 7. SEM Micrographs of zinc deposits with and without additives. (a) BE (b) BE+PVA (c) BE+PVA+VER. (d) BE+PVA+PIP.

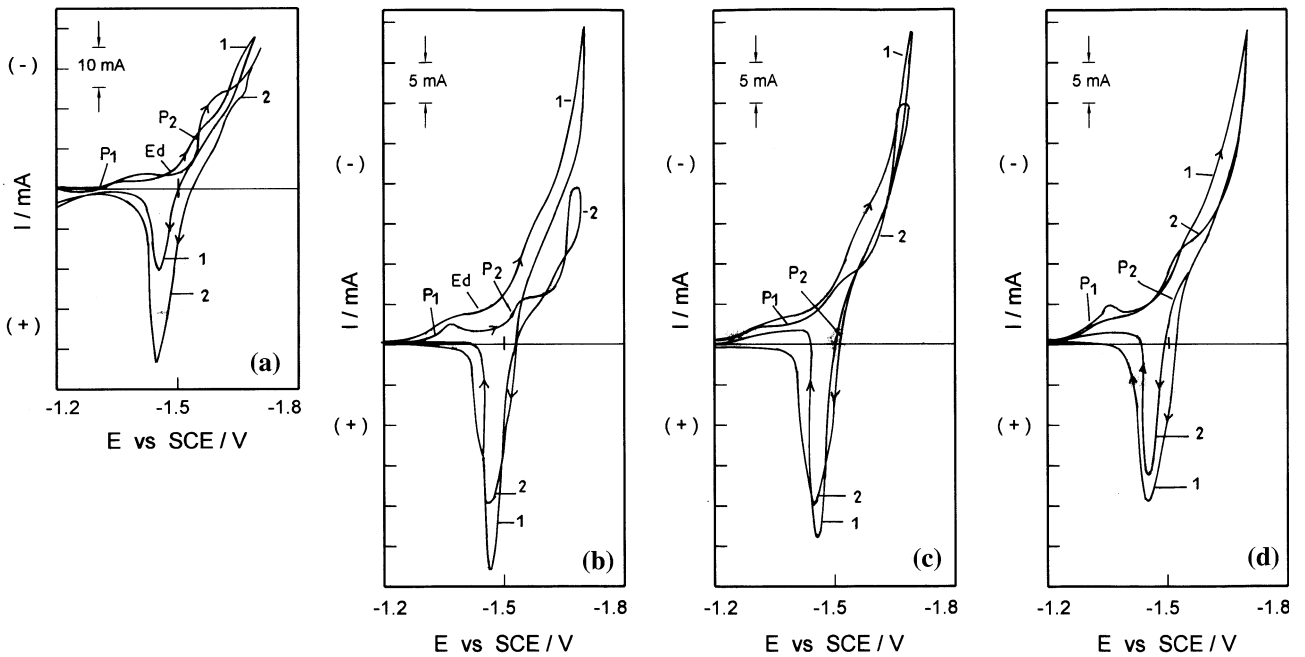


Fig. 8. (a-d). Cyclic voltammogram. (a1) BE+PVA (a2)BE; (b1) BE+PVA (b2) BE+PVA+ANI; (c1) BE+PVA (c2) BE+PVA+VER; (d1) BE+PVA (d2) BE+PVA+PIP.

Table 3. Cyclic voltammetric data

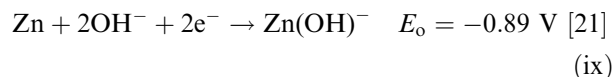
BATH	I_{cp1}/mA	I_{cp2}/mA	E_{cp1}/V	E_d/V	E_{cp2}/V	E_H/V
BE	4	24	1.37	1.48	1.59	1.63
BE + PVA	3	11	1.32	1.48	1.55	1.60
BE + PVA + PIP	3	11	1.36	1.39	1.52	1.56
BE + PVA + VER	2	8.5	1.34	1.4	1.55	1.57
BE + PVA + ANI	2	4.2	1.35	1.45	1.53	1.6

of aldehydes causes additional polarization. The extent of polarization is highest with ANI and lowest with PIP. This trend is also supported by the current efficiency studies.

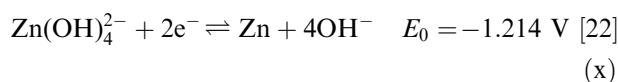
The CV indicates a small peak (p_1) prior to the zinc reduction peak. The formation of two peaks in the presence of additives has already been reported [20]. This should correspond to the reactions



and



The Zinc reduction peak (p_2) corresponds to the reaction



PVA helps in reducing the rate of reaction (ii/v) enabling compact deposition due to the reasons stated above. Addition of PVA decreased E_{p1} , I_{p1} and I_{p2} values due to its high adsorption, but did not alter the E_d value. However, its ability to form a polymer film results in the development of a surface film as deposition proceeds, which not only affects the surface appearance but also inhibits the rate of zinc reduction and causes reduced current efficiency compared to that obtained in the presence of aldehydes. Addition of aldehydes helped to obviate the problem of film formation, which accounts for the increased current efficiency. The additional polarization caused by the aldehydes reduced the I_{p2} value. However, E_d values were reduced by the presence of aldehydes, the maximum reduction being given by PIP.

5. Conclusion

A non-cyanide alkaline bright zinc formulation has been developed to produce deposits similar to those from cyanide baths with respect to brightness and throwing power. The new bath also has the additional advantage

of being eco- friendly in that it uses only easily disposable organics.

Acknowledgement

The authors thank the Director, Central Electrochemical Research Institute, Karaikudi for permission to publish this paper.

References

1. S. Schneider, *Plat. & Surf. Finish.* **89** (2002) 13.
2. B.S. James and W.R. McWhinnie, *Trans. Inst. Met. Finish.* **58** (1980) 72.
3. J. Darken, *Trans. Inst. Met. Finish.* **57** (1979) 145.
4. H. Geduld, *Zincate or Alkaline non-cyanide Zinc Plating in "Zinc Plating"* (ASM International Metals Park, Ohio, 1988), pp. 90–106.
5. M. Schlesinger and M. Paunovic, *Electrodeposition of Zinc and Zinc Alloys in "Modern Electroplating"*, 4th edn., (John Wiley & Sons, New York, 2000), pp. 423–460.
6. L. Oniciu and L. Muresan, *J. Appl. Electrochem.* **21** (1991) 565.
7. J.W. Dini, *Additives in "Electrodeposition – The Materials Science of Coatings and Substrates"* (Noyes Publications, New York, 1993), pp. 195–248.
8. G.A. Hope, G.M. Brown, D.P. Schweinsberg, K. Shimizu and K. Kobayashi, *J. Appl. Electrochem.* **25** (1995) 890.
9. E. Budman, *Met. Finish.* **93** (1995) 60.
10. A. Ramachandran and S.M. Mayanna, *Met. Finish.* **90** (1992) 61.
11. B.S. James US.Pat. 4071418 (1978).
12. W.E. Eckles, W.J. Ferguson and W.J. William. US. Pat. 4188271 (1980).
13. S. Acimovic, K.H. Lindermann and V.G. Gunz. US. Pat. 4166778 (1979).
14. W.E. Roserberg and H.H. Geduld. US Pat. 3803008 (1974).
15. H.G. Crentz US. Pat. 3,853,718 (1974).
16. V. Ravindran, R.M. Krishnan and V.S. Muralidharan, *Met. Finish.* **96** (1998) 10.
17. M. Monev, L. Mirkova, I. Krastev, Hr. Tsvetkova, ST. Rashkov and W. Rightering, *J. Appl. Electrochem.* **28** (1998) 1107.
18. L. Mirkova, M. Monev, I. Krastev and S. Rashkov, *Trans. Inst. Met. Finish.* **73** (1995) 107.
19. G.D. Wilcox and P.J. Mitchell, *Trans. Inst. Met. Finish.* **65** (1987) 76.
20. V.N. Titova, A.A. Javich, N.V. Petrova, V.A. Kazakov and S. Bialozor, *B. Electrochem.* **16** (2000) 425.
21. M. Antleman and F.J. Harmi Jr., *The Encyclopedia of Chemical Electrode potentials* (Plenum Press, New York, 1982), pp. 20–21.
22. G. Caroli and V.K. Sharma, *Table of Standard Electrode Potentials* (John Wiley & Sons, New York, 1978), pp. 95.